

STRONG PIONIC DECAYS OF BARYONS FROM A SPECTROSCOPIC QUARK MODEL

F. Cano, P. González and S. Noguera

Departamento de Física Teórica and IFIC
Centro Mixto Universidad de Valencia - CSIC
46100 Burjassot (Valencia), Spain.

B. Desplanques

Institut des Sciences Nucléaires, F-38026
Grenoble Cedex, France.

Abstract

From a refined non-relativistic quark model that fits the baryonic low-energy spectrum the study of strong pion decay processes within an elementary emission model scheme points out the need of incorporating size-contributing components into the baryon wave functions. In particular the effect of a $(qqq q\bar{q})$ component is investigated in the framework of a quark pair creation model.

Preprint **FTUV/95-71, IFIC/95-74**
Preprint **arch-ive/9606038**

1 Introduction

In QCD, the basic theory of strong interactions (responsible for the hadronic structure), elementary constituents (quarks) which are massless if chiral symmetry is preserved can acquire a dynamically generated mass associated to the spontaneous breakdown of chiral symmetry that takes place when the strong interaction reaches a critical intensity. On the other hand, although not conclusively proved in (3+1) dimensions, QCD seems to be a confining theory. Assuming that the energy scale for the chiral symmetry breaking is higher than the corresponding one for confinement ($\simeq \Lambda_{QCD}$), one gets the image of a baryon as a confined system of interacting massive quarks and Goldstone bosons coming from the symmetry breakdown.

Little more than this qualitative statement can be said from QCD at the current moment since the lack of an adequate method to describe a bound state within a quantum field theory, together with the non-perturbative character of the interaction below Λ_{QCD} , makes difficult any attempt to go further. As a consequence several models of hadronic structure have been developed. Among them perhaps the ones closer related to the image of QCD just drawn are the bag models where the quarks move almost freely inside a confinement region, the bag, surrounded by a mesonic cloud. However the separation of the center of mass motion (indispensable to tackle the problem of baryon structure) added to the fact that one has to simultaneously solve for the movement of the quarks and the bag surface, make the model technically complex. To avoid these difficulties one could wonder whether it would be possible or not to construct an equivalent (regarding the low-energy description) non-relativistic model. Undoubtedly the extensions and refinements from the naive quark model of hadron structure [1] are steps in this direction. In this line De Rújula *et al.* [2] derived an interquark potential from the non-relativistic reduction of the one gluon exchange diagram in QCD to be considered together with the phenomenological confining interaction. The resulting non-relativistic quark model (NRQM) reproduces the image of the quark core of the bag, the mesonic cloud having been obviated. The absence of mesons together with the non-relativistic treatment poses serious doubts about its usefulness unless the incorporation of new terms in the potential and/or the effectiveness of the parameters of the model allows to mitigate at least partially these shortcomings. As an immediate consequence of this way of proceeding, the constituent quarks loose a direct connection to the quark fields of the QCD lagrangian, representing effective degrees of freedom. This viewpoint is also supported by the absence of a strong necessity to introduce in the interaction between quarks some terms issued from the one gluon exchange such as the spin-orbit or tensor forces [3, 4].

The first requirement to such an effective model should be a good description of the hadronic spectrum (at least at low energies) that allows a correct assignment of the theoretical states to the experimental ones. This can be accomplished

with relative success for mesons as well as for baryons by a “minimal” model involving confinement plus part of the one gluon exchange (OGE) potentials [4]. Nevertheless an endemic problem in the low energy spectrum remains, that is the impossibility to correctly predict the masses for the first radial excitations in the baryonic octet and decuplet. The systematic of this wrong prediction led some authors [5] to add a phenomenological three–quark force getting the correct baryonic spectrum (for negative and positive parity states with and without strangeness simultaneously) up to an excitation energy of 0.7 GeV without need to resort to any specific resonance mechanism. This model, that will serve as our starting point now, presents however some conceptual problems which we shall consider firstly.

The second requirement is the correct description of the baryon properties, what involves the wave functions of the baryons on the one hand, the operator relative to the process under discussion on the other hand. Having a model that correctly describes the low energy baryonic spectrum, it is appropriate to compare its predictions to those of other models that do not do so well for the baryon masses. This may allow us to determine whether there is some bias to be introduced in the comparison to experiments due to a poor prediction of baryon masses (though some discrepancy may be due to different physical ingredients). This comparison was our main intent originally for looking at the strong pion decays of baryons. It however appeared that results were very much sensitive to the microscopic description of the process. This led us to examine various aspects of the problem, where relativity is often present in one way or another. The present work is part of a general program tending to extract from the comparison of the models to each other and to the data some general features of the “true” wave functions that in their turn should serve as a guide to further refinements of the models themselves. The contents of the presentation are organized hereforth as follows. In section 2 we review the quark models we make use of and their predictions for static properties. In sections 3 and 4 we study strong pion decay processes within two different approaches, namely the elementary emission model (EEM) and the quark pair creation model (QPCM) that we modify in order to correct its energy dependence. Finally in section 5 we summarize our main conclusions

2 The Quark Models

The non–relativistic quark model of hadron structure describes the hadron (color singlet bound state) in terms of a definite number of components (constituent quarks q , and antiquarks \bar{q}) that interact through an effective potential. The analysis of the mesonic ($q\bar{q}$) and baryonic (qqq) spectrum leads to a minimum two–body potential containing the basic QCD motivated, confining, coulombic (OGE) and spin–spin (OGE) qq interactions, of the form:

$$V_I = \frac{1}{2} \sum_{i < j} \left(-\frac{\kappa}{r_{ij}} + \frac{r_{ij}}{a^2} + \frac{\kappa_\sigma}{m_i m_j} \frac{\exp -r_{ij}/r_0}{r_0^2 r_{ij}} \vec{\sigma}_i \vec{\sigma}_j - D \right) \quad (1)$$

where D is a constant to fix the origin of the potential, r_{ij} is the distance between quarks i and j and σ denote the Pauli matrices. The Yukawa form of the spin-spin term replace the $\delta(\vec{r})$ contact interaction of the OGE potential [2] to avoid an unbounded spectrum when solving the Schrödinger equation [6]. The mass parameters $m_{i,j}$ are chosen to fit the baryon magnetic moments and the three parameters a^2 , $\kappa = \kappa_\sigma$, r_0 , fitted from the meson spectrum [4] (see table 1) provide a good description of the baryonic octet and decuplet [4], a part of which is reproduced in fig. 1. A look at this figure makes clear a general deficiency in the description: the masses of the positive parity excitations that correspond to radial excitations of the totally symmetric spatial components of the wave function are systematically higher (from 200 to 400 MeV) than the experimental ones. Any attempt to correct this situation by a refitting of the parameters causes undesirable effects on the rest of the spectrum. Then the open question refers to the possibility of solving the problem by means of the introduction of some physically founded new term in the potential.

Attending the mixed symmetric spatial structure of the first negative parity excitations it becomes obvious that they will be much less affected by an interaction tending to group the three quarks than the spatially symmetric ground states and its first radial excitations. Having in mind a genuine three quark interaction as the exchange of two sigma mesons at the same point, Desplanques *et al.* [5] proposed a three-body potential

$$V_{II}^{(3)} = \frac{1}{2} \sum_{i \neq j \neq k \neq i} \frac{V_0}{m_i m_j m_k} \frac{e^{-m_0 r_{ij}}}{m_0 r_{ij}} \frac{e^{-m_0 r_{ik}}}{m_0 r_{ik}} \quad (2)$$

The low energy baryonic spectrum can be then well reproduced with a 'two plus three body' interaction:

$$V_{II} = V_{II}^{(2)} + V_{II}^{(3)} \quad (3)$$

where $V_{II}^{(2)}$ differs from V_I in the values of the parameters. As a consequence the unified description of both the mesons and baryonic spectra given by V_I is lost. More than a drawback one should consider this as the natural outcome of the effectiveness of the parameters (through them for instance, some mesonic effects, only present in the baryonic case might be incorporated).

The form used in ref. [5] for the potential, eq. (3), shows some non-appealing features. Concerning the two-body piece $V_{II}^{(2)}$, the range of the spin-spin interaction, $r_0 = 1.28$ fm, needed in [5] is very far from the one which could reasonably be expected given the original $\delta(\vec{r})$ form of this interaction [2]. This comes from the minimum number of parameters' constraint $\kappa = \kappa_\sigma$. Nevertheless one can get a

much more “reasonable” range (0.4 fm) without increasing the number of parameters by recovering the original OGE potential relation between the coulombian intensity κ ($\kappa = -\frac{4}{3}\alpha_s$) and the spin–spin one κ_σ ($\kappa_\sigma = -\frac{2}{9}\alpha_s$), i.e. $\kappa_\sigma = \frac{1}{6}\kappa$. The resulting value of r_0 might represent somehow an effective average between 0 fm, the OGE δ –term range, and ≈ 1 fm, the range of the quark pionic exchange not implemented in our model. This impression seems to be reinforced by the corresponding value of the effective QCD coupling constant, $\alpha_s \approx 1$, that doubles the one needed in models where pionic quark exchanges are explicitly incorporated [8].

From now on we shall call V_{II} the two plus three body interaction with $V_{II}^{(2)}$ corrected as explained. The fit to the spectrum with this corrected potential (see table 1) a part of which is reproduced in fig. 2, hardly differs from that in ref [5].

Regarding the 3–body piece of the interaction (3), $V_{II}^{(3)}$, its long range, 0.8 fm, can find a justification attending the small value of the coefficient of the linear potential (or equivalently its small contribution to the string tension). For higher angular momentum states where the quarks are very far apart, the long range of $V_{II}^{(3)}$ would allow a contribution to the string tension to explain the leading Regge trajectories. It is difficult however to justify if we think of the three nucleon force this 3–quark term would give rise to. To correct for this behaviour a less singular form of the interaction is required. For the sake of technical simplicity we shall adopt here a gaussian form

$$V_{III}^{(3)} = V_0 \exp\left(-\sum_{i<j} \frac{r_{ij}^2}{\lambda^2}\right) \quad (4)$$

very easy to be used in the hyperspherical harmonic formalism (Appendix A) [9] we work with.

The parameters of the potential

$$V_{III} = V_{III}^{(2)} + V_{III}^{(3)} \quad (5)$$

appear in table 1 (note that the range of $V^{(3)}$ has gone down to 0.25 fm and that we have relaxed the constraint between κ and κ_σ), and the comparative spectrum, of similar quality to the V_{II} ’s one, appears (in part) in fig. 3.

With regard to other parameters of the potential some comments are in order. For the quark masses, m_u , m_d , a value between 300 and 360 MeV, that fits the nucleon magnetic moments (assuming an SU(6) spatially symmetric wave function) within a 10 % of error, is generally accepted. It can be shown (Appendix A) that, from the potential we are dealing with, one can obtain via an adequate redefinition of the parameters of the potentials, a non–strange energy spectrum (for quark mass m') whose energies, E' , are related to the initial ones E (for quark mass m) by

$$E' = \frac{m}{m'}E \quad (6)$$

and with no other change than a distance rescaling in the wave functions. Hence given a fit to the spectrum for a given quark mass, eq. (6) gives the shifted relative energies when changing the quark mass, i.e. the baryon magnetic moment.

The strength of the confining term is considerably reduced due to the presence of the three body force (see table 1). This gives rise to a grouping of the states in the 'high' energy part of the spectrum that could be suggesting the need of some qualitative change in the three-body or in the confinement pieces. Nevertheless the lack of precise experimental information in this region together with the very probable presence of significant relativistic effects prevent us from extracting quantitative conclusions from it.

Once, via the fit of the spectrum, some physical states are unambiguously ascribed to model states (up to 0.7 GeV excitation energy) we should focus on the description of the baryonic properties. As explained before the nucleon magnetic moments are reasonably well reproduced (see table 2) with masses between 300 and 360 MeV indicating the dominance of the spatially symmetric component of the wave function (see fig. 4). A different case is the mass and charge root mean square radius (r.m.s.). For the nucleon charge radius for instance the predicted values are too low compared to the data. This can be understood by taking into account that our effective scheme only incorporates the description of the core of quarks, whose pretty small size has to do with the pressure exerted by the mesonic cloud that in our meson-absent models is simulated through the effective values of the parameters. Then, if the mesonic contribution to the total mass is small as compared to the core contribution (as it happens to be the case in the bag models), one can understand the r.m.s.-spectrum puzzle, i.e. the impossibility within a model scheme that only plays with effective quark degrees of freedom of simultaneously fitting the spectrum and the total sizes.

Furthermore the absence of $(qqq q\bar{q})$ components in the wave function should be at least in part also responsible for the high values $(5/3)$ predicted for the axial coupling constant g_A as it is suggested by bag model calculations [10].

As a corollary it may be established that when dealing with physical processes where the mesonic cloud plays a relevant role as such the use of a spectroscopic quark model requires the use of effective operators that can give account of it. Hence for the strong pion decay we consider next a careful analysis of the transition matrix elements is needed before a comparison between different spectroscopic quark models makes any sense.

3 The Elementary Emission Model (EEM)

To study strong baryonic decays we shall follow the elementary emission model approach developed long time ago [11]. The decay takes place through the emis-

sion of a point-like pion by one of the quarks of the baryon (fig. 5) and therefore the coupling constant is unique for all the processes.

Up to order $(\frac{p_q}{m_q})$ the matrix elements for the process $B \rightarrow B'\pi$ can be expressed as $\langle B'|H|B\rangle$ [12] with

$$H = -\frac{3i}{(2\pi)^{3/2}} \frac{1}{(2\omega_\pi)^{1/2}} \frac{f_{qq\pi}}{m_\pi} (\tau^\alpha)^{\dagger(3)} \left[\vec{\sigma}^{(3)} \vec{k} e^{-i\vec{k}\vec{r}_3} - \frac{\omega_\pi}{2m_q} \left\{ \vec{\sigma}^{(3)} \vec{p}^{(3)}, e^{-i\vec{k}\vec{r}_3} \right\} \right] \quad (7)$$

where the factor 3 comes from the number of quarks, ω_π and \vec{k} stand for the pion energy and trimomentum respectively and \vec{r}_3 is the quark 3 coordinate. The upper index (3) on the operators of spin, $\vec{\sigma}$, isospin, τ , and quark trimomentum, \vec{p} , indicates that we have chosen for later technical simplicity the quark 3 to perform the calculations. The coupling constant $f_{qq\pi}$ is related to the usual $g_{qq\pi}$ through the quark-pion mass ratio:

$$\frac{f_{qq\pi}}{m_\pi} = \frac{g_{qq\pi}}{2m_q} \quad (8)$$

and is the only free parameter of the model.

The ‘non-relativistic’ $qq\pi$ interaction given by H may be obtained from the $qq\pi$ invariant interaction with the pseudovector coupling $\mathcal{L}_{qq\pi} \simeq \bar{\Psi}_q \vec{\tau} \gamma_\mu \gamma_5 \Psi_q \partial^\mu \vec{\pi}$. It differs from that obtained with the pseudoscalar coupling $\mathcal{L}_{qq\pi} \simeq \bar{\Psi}_q \vec{\tau} \gamma_5 \Psi_q \vec{\pi}$ since at first order in $(\frac{p}{m})$, this one does not give rise to the term proportional to ω_π in eq. (7) (it only gives the $\vec{\sigma}\vec{k}$ term). The examination of the higher order terms in $(\frac{p}{m})$ in the pseudoscalar coupling case shows that there are some $(\frac{p}{m})^2$ corrections to the $\vec{\sigma}\vec{k}$ term which are identical to those that would be derived in the pseudovector coupling. As an expansion in $(\frac{p}{m})^2$ is meaningless in view of the large value taken by this quantity (larger than 1, with often a destructive interference at the first order) we prefer to freeze these p^2 terms and replace them by some constant. In practice, this means that they will be hidden in the coupling $f_{qq\pi}$ to be fitted to reproduce the $f_{NN\pi}$ coupling. The other $(\frac{p}{m})^2$ corrections in the pseudoscalar coupling represent the difference in the kinetic energies of quarks in the initial and final states, which enters in ω_π ($\omega_\pi = E_B - E_{B'}$). The difference in potential energies in the initial and final states, which is also included in ω_π , is provided by terms involving the excitation of a quark-antiquark pair (this one is known to be important in the pseudoscalar coupling).

Notwithstanding that it corresponds to a higher order term in $(\frac{p}{m})$ in the pseudoscalar coupling, we shall maintain the term proportional to ω_π in eq. (7), because of its different functional structure. Altogether, eq. (7) amounts to retain for the different types of terms, $\vec{\sigma}\vec{k}$ and $\vec{\sigma}\vec{p}$, corresponding to the lowest order

contributions in $(\frac{p}{m})$, relativistic corrections being embedded in the parameter $f_{qq\pi}$ or in the factor ω_π itself.

In order to evaluate the matrix elements of the hamiltonian H the wave function of a baryon of spin J and third component J_z is factorized as a plane wave of trimomentum \vec{P} (the baryon trimomentum) for the center of mass motion multiplied by the intrinsic wave function, i.e.

$$|B\rangle = \frac{1}{(2\pi)^{3/2}} e^{i\vec{P}_B \vec{R}} \left[\Psi_B(\vec{\xi}_1, \vec{\xi}_2) \Phi_B(S, M_S; I, M_I) \right]_{JJ_z} \quad (9)$$

where Φ_B stands for the spin–isospin part and Ψ_B is the spatial internal wave function in terms of the Jacobi coordinates $\vec{\xi}_1, \vec{\xi}_2$.

Then the amplitudes for the decay, defined by:

$$J', \lambda \langle B' | H | B \rangle_{J, \lambda} = \frac{1}{(2\pi)^{3/2}} \delta(\vec{P}_B - \vec{P}_{B'} - \vec{k}) A_\lambda^{(i,f)} \quad (10)$$

where i and f refer to the internal quantum numbers of the initial and final baryons, are given by:

$$\begin{aligned} A_\lambda^{(i,f)} = & -\frac{3i}{(2\omega_\pi)^{1/2}} \frac{f_{qq\pi}}{m_\pi} \int d\vec{\xi}_1 \int d\vec{\xi}_2 \left[\Psi_{B'}(\vec{\xi}_1, \vec{\xi}_2) \Phi_{B'}(M', M'_S; I', M'_I) \right]_{J'\lambda}^* \\ & (\tau^\alpha)^{\dagger(3)} \left[\vec{\sigma}^{(3)} \vec{k} \left(1 + \frac{\omega_\pi}{6m_q} \right) e^{i\sqrt{\frac{2}{3}} \vec{k} \vec{\xi}_2} \right. \\ & \left. - \frac{\omega_\pi}{2m_q} \left\{ \vec{\sigma}^{(3)} \left(-\sqrt{\frac{2}{3}} \vec{p}_{\xi_2} + \frac{\vec{P}_B}{3} \right), e^{i\sqrt{\frac{2}{3}} \vec{k} \vec{\xi}_2} \right\} \right] \\ & \left[\Psi_B(\vec{\xi}_1, \vec{\xi}_2) \Phi_B(S, M_S; I, M_I) \right]_{J\lambda} \end{aligned} \quad (11)$$

The dependence on \vec{P}_B may suggest a dependence of the amplitudes on the frame of reference. In the present case, the corresponding term combines with the first term proportional to \vec{k} in eq. (11) to get a term proportional to $\vec{k} - \frac{\omega_\pi}{3m_q} \vec{P}_B$ ($\simeq \vec{k} - m_\pi \frac{\vec{P}_B}{M_B}$) in the non relativistic limit), which ensures the Galilean invariance of the amplitude at the lowest order in $\frac{\omega_\pi}{M_B}$. This invariance of the amplitude at the quark level was imposed by Mitra and Ross [13] to introduce in the $qq\pi$ interaction some ω_π dependent term, quite similar to the one in eq. (7). We shall work in the frame where the decaying resonance is at rest ($\vec{P}_B = \vec{0}$). For later purpose it is convenient to reexpress the amplitudes in the more compact form:

$$A_\lambda = -\frac{3i}{(2\omega_\pi)^{1/2}} \frac{f_{qq\pi}}{m_\pi} \left\{ \left(1 + \frac{\omega_\pi}{6m_q} \right) N_{i,f} - \frac{\omega_\pi}{2m_q} R_{i,f} \right\} \quad (12)$$

The notation $N_{i,f}$, $R_{i,f}$ is a technical one. R includes derivatives (coming from the momentum operator \vec{p}_{ξ_2}) whereas N does not. They are directly related

to the more physical recoil (depending on the recoil momentum $(\vec{p}^{(3)} - \vec{k})$) and direct (depending of the pion momentum \vec{k}) contributions.

Finally the decay width is obtained from the amplitudes in the initial baryon (B) rest frame as [12]:

$$\Gamma_{B \rightarrow B' \pi} = \frac{1}{2\pi} \frac{E_{B'} \omega_\pi}{m_B} k \overline{\sum_{\lambda, i, f}} |A_\lambda^{(i, f)}|^2 \quad (13)$$

where the overline indicates the average over the initial spin–isospin. The kinematical magnitudes and the baryon masses depend on the spectroscopic model, so that for V_{II} and V_{III} they are pretty close to the experimental ones, whereas for V_I the difference (especially for the Roper decays) can be very significant. Nevertheless as we shall be interested (once the transition operator has been chosen) in testing the baryonic wave functions we shall use the same kinematics, i.e. the experimental values of m_B , $E_{B'}$, ω_π and \vec{k} , in all our calculations.

3.1 Fitting of $f_{qq\pi}$

There is no unique criterium in the literature to fix $f_{qq\pi}$. For instance $f_{qq\pi}$ could be chosen to get the best global fit to the data [14]. Nonetheless, for the purpose of analyzing the baryonic wave function another possibility is more convenient, namely to fit $f_{qq\pi}$ to reproduce the $NN\pi$ interaction at low momentum transfers. Thus we compare the matrix element for the process $p \uparrow \rightarrow p \uparrow \pi^0$ calculated at the quark level from H, eq. (7), with the same matrix element at baryonic level obtained from:

$$H_{\text{Bar}} = -\frac{i}{(2\pi)^{3/2}} \frac{1}{(2\omega_\pi)^{1/2}} \frac{f_{NN\pi}(k)}{m_\pi} (\tau_N^\alpha)^\dagger \left[(\vec{\sigma}_N \vec{k}) e^{-i\vec{k}\vec{R}} - \frac{\omega_\pi}{2m_N} \left\{ \vec{\sigma}_N \vec{P}_N, e^{-i\vec{k}\vec{R}} \right\} \right] \quad (14)$$

By assuming the nucleon to be a totally symmetric spin–isospin SU(6) state (the mixed–symmetric component of the nucleon has less than 2 % probability for our quark models) one gets:

$$f_{NN\pi}(k) = f_{qq\pi} \frac{5}{3} \frac{\left(1 + \frac{\omega_\pi}{6m_q}\right)}{\left(1 + \frac{\omega_\pi}{2m_N}\right)} F(k) \quad (15)$$

where $F(k = |\vec{k}|)$ contains all the information about the spatial structure of the nucleon as provided by the quark model. Explicitly:

$$F(k) = \frac{12}{k^2} \mathcal{I}_{N_1 N_1}^{3,2}(k) \quad (16)$$

where \mathcal{I} represents an integral of the general form:

$$\mathcal{I}_{B_i C_j}^{l,m}(k) = \int d\xi \xi^l \Psi_{B_i}^*(\xi) J_m(\sqrt{\frac{2}{3}} k \xi) \Psi_{C_j}(\xi) \quad (17)$$

J_m standing for the Bessel function of order m and Ψ_{B_i} (Ψ_{C_j}) for the hyperradial part of the wave function for the i (j) channel of baryon B (C).

In the limit ($\vec{k} \rightarrow 0$, $\omega_\pi = m_\pi$), the spatial structure reduces to $F(k) \rightarrow 1$, and then

$$f_{qq\pi} = \frac{3}{5} \frac{f_{NN\pi}(0)}{B(m_\pi)} \quad (18)$$

having defined

$$B(x) = \frac{(1 + \frac{x}{6m_q})}{(1 + \frac{x}{2m_N})} \quad (19)$$

Hence the only dependence of $f_{qq\pi}$ on the spectroscopic model comes from the non-relevant quark mass differences, having the values $f_{qq\pi} = 0.602, 0.604, 0.600$ for V_I, V_{II} and V_{III} respectively ($f_{NN\pi} = 0.998$).

Once $f_{qq\pi}$ has been fitted in this almost model independent manner, the predictions of the models serve as a test, within a EEM scheme, of the baryonic wave functions. For instance, by writing $f_{NN\pi}$ in terms of a normalized form factor $G(k)$:

$$f_{NN\pi}(k) = f_{NN\pi}(0)G(k) \quad (20)$$

with $G(k=0, \omega_\pi = m_\pi) = 1$, we have

$$G(k) = F(k) \frac{B(\omega_\pi)}{B(m_\pi)} \quad (21)$$

The results appear in fig. 6, against the phenomenological parameterization of ref. [15]. As can be seen neither V_{II} nor V_{III} provide with a good form factor (although the deviation is at most of a 10 % for small k values). The reason for it is clear when making an expansion in powers of k :

$$G(k) = 1 - \frac{1}{6} k^2 \langle r^2 \rangle + \dots \quad (22)$$

Thus for the small values of k one is directly testing the root mean square mass radius:

$$\langle r^2 \rangle = \left\langle \frac{\sum_{i=1}^3 m_i (\vec{r}_i - \vec{R})^2}{\sum_{i=1}^3 m_i} \right\rangle = \frac{1}{3} \langle \xi^2 \rangle \quad (23)$$

which turns out to be too small for V_{II} and V_{III} . This is not certainly a surprise from our considerations in section 2 since it can be an indication that relativistic effects, pionic components ($qqq q\bar{q}$), etc may be playing a role. Alternatively it may be suggesting the need to refine the three-body potential.

3.2 Strong pion decays

To pursue the analysis of the wave functions, within the EEM, we evaluate the widths for strong pion decays of nucleon and delta resonances. The results are listed in table 3. Although it is difficult to extract general features from them (the almost zero widths for the processes involving the ground state and its first radial excitation, $N(1440) \rightarrow N\pi$ and $\Delta(1600) \rightarrow \Delta\pi$, comes from the orthogonality of their radial wave functions) we can say that for decays clearly dominated by the non-derivative part of the amplitude ($N(1520) \rightarrow N\pi$, $\Delta(1232) \rightarrow N\pi$) the three potentials work reasonably well, the better the result the bigger the predicted radius for the nucleon. This comes along the same line that our previous discussion for the $NN\pi$ form factor since the non-derivative terms involve the average wave function overlap. In order to try to include size contributing components, we shall explore next the possibility of incorporating the pion structure in a non-relativistic scheme.

4 The Quark Pair Creation Model (QPCM)

To implement the mesonic structure several formalisms have been developed [12], all of them sharing the image of the meson emission as the creation of a $q\bar{q}$ pair that by later recombination gives rise to the outgoing meson.

At the effective level we work, the choice of one or other QPCM comes mainly motivated by simplicity. In this sense the 3P_0 QPCM is manageable and comparable in the limit of point pion to the EEM. Schematically the process is pictured in fig. 7. The $q\bar{q}$ pair created has the quantum numbers of the vacuum: flavor and color singlet, zero momentum and total angular momentum $J^{PC} = 0^{++}$ ($\Rightarrow L = 1, S = 1$). This translates into a transition operator:

$$T = - \sum_{i,j} \int d\vec{p}_q d\vec{p}_{\bar{q}} \left[3\gamma \delta(\vec{p}_q + \vec{p}_{\bar{q}}) \sum_m (110|m, -m) \mathcal{Y}_1^m(\vec{p}_q - \vec{p}_{\bar{q}}) \mathcal{Z}_{i,j}^{-m} \right] b_i^\dagger(\vec{p}_q) d_j^\dagger(\vec{p}_{\bar{q}}) \quad (24)$$

where γ is the (dimensionless) parameter strength of the model, \mathcal{Y}_L^M is a solid harmonic and $\mathcal{Z}_{i,j}^{-m}$ contains the color-spin-isospin wave function of the pair. The matrix element for the process $B \rightarrow B'M$ is then written as:

$$\langle B'M|T|B\rangle = -3\gamma \sum_m (110|m, -m) \langle \Phi_{B'} \Phi_M | \Phi_B \Phi_{\text{pair}}^{-m} \rangle I_m(B; B'M) \quad (25)$$

where Φ stands for the spin–isospin wave function and

$$\begin{aligned} I_m &= \int d\vec{p}_1 d\vec{p}_2 d\vec{p}_3 d\vec{p}_4 d\vec{p}_5 \mathcal{Y}_\infty^\dagger(\vec{\nabla}_\Delta - \vec{\nabla}_\nabla) \delta(\vec{\nabla}_\Delta + \vec{\nabla}_\nabla) \cdot \\ &\quad \Psi_{B'}^*(\vec{p}_1, \vec{p}_2, \vec{p}_4) \Psi_M^*(\vec{p}_3, \vec{p}_5) \Psi_B(\vec{p}_1, \vec{p}_2, \vec{p}_3) \\ &= \frac{1}{(2\pi)^{3/2}} \delta(\vec{P}_B - \vec{P}_{B'} - \vec{k}) \int d\vec{\xi}_1 d\vec{\xi}_2 d\vec{\xi}_2' \Psi_{B'}^*(\vec{\xi}_1, \vec{\xi}_2') O(\vec{\xi}_2', \vec{\xi}_2) \Psi_B(\vec{\xi}_1, \vec{\xi}_2) \end{aligned} \quad (26)$$

the kernel $O(\vec{\xi}_2', \vec{\xi}_2)$ being the non–local operator:

$$\begin{aligned} O(\vec{\xi}_2', \vec{\xi}_2) &= 3\mathcal{Y}_1^m \left(-\sqrt{\frac{2}{3}}(\vec{p}_{\xi_2} + \vec{p}_{\xi_2}') - \frac{4}{3}\vec{k} + \frac{2}{3}\vec{P}_B \right) \Psi_M^* \left(\sqrt{\frac{3}{2}}(\vec{\xi}_2' - \vec{\xi}_2) \right) \\ &\quad \exp \left(i\sqrt{\frac{3}{2}}\vec{P}_B(\vec{\xi}_2' - \vec{\xi}_2) \right) \exp \left(i\sqrt{\frac{1}{24}}\vec{k}(\vec{\xi}_2' - \vec{\xi}_2) \right) \exp \left(i\sqrt{\frac{2}{3}}\vec{k}\vec{\xi}_2 \right) \end{aligned} \quad (27)$$

in terms of the meson wave function Ψ_M .

Let us note that, in the rest frame of the decaying baryon ($\vec{P}_B = 0$) we recover in the limit of a point–like meson $\Psi_M(\sqrt{\frac{3}{2}}(\vec{\xi}_2' - \vec{\xi}_2)) \rightarrow (2\pi)^{3/2} \sqrt{\frac{2}{3}} \delta(\vec{\xi}_2' - \vec{\xi}_2)$ the operational structure of the EEM (see eqs. 10 and 11), say

$$\begin{aligned} \langle B'M|T|B\rangle &\rightarrow \frac{1}{(2\pi)^{3/2}} \delta(\vec{P}_B - \vec{P}_{B'} - \vec{k}) (-\gamma 3\sqrt{3}\pi) \langle \Phi_{B'} \Phi_M | \Phi_B \vec{\Phi}_{\text{pair}} \rangle \\ &\quad \int d\vec{\xi}_1 d\vec{\xi}_2 \Psi_{B'}^*(\vec{\xi}_1, \vec{\xi}_2) \left[\frac{4}{3}\vec{k} e^{i\sqrt{\frac{2}{3}}\vec{k}\vec{\xi}_2} + \sqrt{\frac{2}{3}} \left\{ \vec{p}_{\xi_2}, e^{i\sqrt{\frac{2}{3}}\vec{k}\vec{\xi}_2} \right\} \right] \Psi_B(\vec{\xi}_1, \vec{\xi}_2) \end{aligned} \quad (28)$$

Hence it is obvious that we reproduce the EEM amplitudes by making in eq. (11) the replacements:

$$\frac{\omega_\pi}{2m_q} \rightarrow 1 \quad (29)$$

$$\frac{3if_{qq\pi}}{(2\omega_\pi)^{1/2}m_\pi} \rightarrow \gamma 3\sqrt{3} \frac{\pi}{4} \quad (30)$$

In other words the compositeness of the meson reflects, with regard to the EEM, not only through the meson wave function but also in the transition operator.

For the pion wave function we shall make use of a gaussian form fitted ($R_A = 8 \text{ GeV}^{-2}$) to reproduce the root mean square radius of the pion [16]:

$$\Psi_\pi(\vec{r}) = \frac{1}{(\pi R_A^2)^{3/4}} \exp\left(-\frac{\vec{r}^2}{2R_A^2}\right) \quad (31)$$

With an orientative purpose we compare it with the wave function extracted from the knowledge of the electromagnetic pion form factor for which (at low Q^2) we can very approximately assume vector meson (ρ -meson) dominance [17]:

$$F_\pi(Q^2) = \frac{m_\rho^2}{m_\rho^2 + Q^2} \quad (32)$$

The Fourier transform of $F_\pi(Q^2)$ gives the charge density from which the pion wave function can be derived:

$$\Psi_\pi(\vec{r}) = Y_{00}(\hat{r}) \frac{m_\rho}{r^{1/2}} \exp\left(-\frac{m_\rho r}{2}\right) \quad (33)$$

We should keep in mind however that this expression is meaningful only at long distances

In fig. 8 we draw the two normalized pion wave functions where the very different short-distance behaviour can be appreciated.

4.1 The normalized $NN\pi$ form factor

To get the normalized form factor defined previously in eq. (20), we compare the matrix element for $p \uparrow \rightarrow p \uparrow \pi^0$ calculated from H_{Bar} (eq. 14) with the one provided by the QPCM, (eq. 25). The results appear in fig. 9. According to our expectations the inclusion of the pion structure seems to play the same role that the increasing of the baryonic size in the EEM model. In this sense half of the difference between the theoretical and the phenomenological results has been corrected for V_{II} and V_{III} (for V_I the quantitative change is not very relevant).

4.2 Fitting of γ

Although the formal replacement in (30) establishes a relationship between $f_{qq\pi}$ and γ it should be handled with care since it is only valid in the point-like limit. If we extract γ from $f_{NN\pi}(0)$ in the same way as we did to get $f_{qq\pi}$ we have:

$$\frac{i}{(2m_\pi)^{1/2}} \frac{f_{NN\pi}(0)}{m_\pi} \left(1 + \frac{m_\pi}{2m_N}\right) = \frac{15}{12\pi^3} \gamma I(0) \quad (34)$$

where

$$I(0) = \int d\xi d\xi' d\phi d\hat{\xi}_2 d\hat{\xi}'_2 \cos^2\phi \sin^2\phi \sqrt{\xi'^2 - \xi^2 \sin^2\phi} \xi^5 \xi' \Theta\left(1 - \frac{\xi \sin\phi}{\xi'}\right).$$

$$\Psi_\pi(a) \left[-\frac{2}{3} \Psi_{N_1}(\xi) \Psi_{N_1}(\xi') - \frac{1}{12} \left(3\xi \cos\theta_2 \cos\phi + \xi' \cos\theta'_2 \sqrt{1 - \left(\frac{\xi \sin\phi}{\xi'} \right)^2} \right) \cdot \right. \\ \left. \left(\cos\theta_2 \cos\phi \Psi'_{N_1}(\xi) \Psi_{N_1}(\xi') - \cos\theta'_2 \sqrt{1 - \left(\frac{\xi \sin\phi}{\xi'} \right)^2} \Psi'_{N_1}(\xi') \Psi_{N_1}(\xi) \right) \right] \quad (35)$$

Θ is the Heaviside step function and the argument of the pion wave function is

$$a = \xi^2 \cos 2\phi + \xi'^2 - 2\xi \cos\phi \sqrt{\xi'^2 - \xi^2 \sin^2\phi} (\hat{\xi}_2 \hat{\xi}'_2) \quad (36)$$

This gives for γ the values shown in table 4. We observe for V_I a quite different value of γ than for V_{II} and V_{III} . This comes about due to the introduction of the pion structure; in the EEM model the constancy of $f_{qq\pi}$ had to do with the fact that the baryonic quark structure contributes through model independent normalization integrals whereas in the QPCM case the presence of the pion wave function weights in a different form the quark structures giving provoking a model dependence in γ that reflects the very different quark–model baryon wave functions, with and without three–quark force. Concerning the pion wave function its very short distance behaviour seems to affect the results very little. It turns out that this will also be the case for strong pion decays. For this reason we shall restrict hereforth our presentation to the gaussian wave function eq. (31). Let us notice that the values of γ available in the literature are much lower than ours, the difference coming from the quark model used (harmonic oscillator) and from having fitted γ in a different way. In ref. [16] the vertex $NN\pi$ was calculated analytically with the harmonic oscillator model. By choosing a value of $R_A^2 = 8 \text{ GeV}^{-2}$ for the pion wave function and a nucleon r.m.s. $R_N^2 = 6 \text{ GeV}^{-2}$ (very close to the one obtained with V_I) the constant γ would be 6.29 (6.97 with V_I).

4.3 Strong Pion Decays

The widths obtained with the 3P_0 model appear in table 5. We see that the introduction of the pion structure does not seem to represent any improvement of the results but rather on the contrary a worsening of the fit.

As the specific form of the pion wave function is not very relevant we center our attention in the transition operator. Possible corrections to it may have a relativistic origin and can be enforced on the basis of general principles. First there is a normalization factor $\sqrt{\frac{m_\pi}{\omega_\pi}}$ which is related to the boost of the pion from its rest frame to the rest frame of the initial baryon. On the other hand, if one desires the quark momentum term to have the same properties as the \vec{k} dependent one under exchanging the role of initial and final states it has to be associated to the difference of the energies of the initial and final states, which is

nothing but ω_π . In the non-relativistic limit, this factor tends to $2m_q$ and it is therefore natural to introduce the factor $\frac{\omega_\pi}{2m_q}$ in front of the momentum term.

This considerations can be implemented in eq. (27) by introducing a factor $\sqrt{\frac{m_\pi}{\omega_\pi}}$ and by multiplying the momentum ($\vec{p}_{\xi_2} + \vec{p}_{\xi'_2}$) dependent term by $\frac{\omega_\pi}{2m_q}$. Actually by making the additional replacement of the \vec{k} coefficient $\frac{4}{3}$ by $\left(1 + \frac{\omega_\pi}{6m_q}\right)$ these changes are equivalent to modify the QPCM to get as the point pion limit the EEM. Adopting this point of view we define our 3P_0 modified QPCM through the operator:

$$\begin{aligned}
O_{\text{mod}}(\vec{\xi}'_2, \vec{\xi}_2) &= 3\sqrt{\frac{m_\pi}{\omega_\pi}} \mathcal{Y}_1^m \left(-\frac{\omega_\pi}{2m_q} \sqrt{\frac{2}{3}} (\vec{p}_{\xi_2} + \vec{p}_{\xi'_2}) - \left(1 + \frac{\omega_\pi}{6m_q}\right) \vec{k} + \frac{2}{3} \vec{P}_B \right) \cdot \\
&\Psi_M^* \left(\sqrt{\frac{3}{2}} (\vec{\xi}'_2 - \vec{\xi}_2) \right) \exp \left(i \sqrt{\frac{3}{2}} \vec{P}_B (\vec{\xi}'_2 - \vec{\xi}_2) \right) \cdot \\
&\exp \left(i \sqrt{\frac{1}{24}} \vec{k} (\vec{\xi}'_2 - \vec{\xi}_2) \right) \exp \left(i \sqrt{\frac{2}{3}} \vec{k} \vec{\xi}_2 \right) \quad (37)
\end{aligned}$$

By repeating the calculational process as explained in section 4.1 and 4.2 the improvement of the fit with this modified QPCM is spectacular as seen in table 6 (the normalized form factor hardly changes and we do not draw it again). Except for $\Delta(1600) \rightarrow N\pi$ and $N(1535) \rightarrow \Delta\pi$ where the strong cancellation between derivative and non-derivative terms makes the result very sensitive to their precise values all the widths are reproduced withing a factor 2. (Let us remark that the experimental interval has been taken as the most-restrictive one, i.e. by applying the corresponding variable decay percentage to the central value of the width).

The results for the transitions involving the nucleon (or Δ particle) and its radial excitations, $N(1440)$ (or $\Delta(1600)$) should be noticed. The finite size of the pion makes them sizeable and in rough agreement with experiment. This is achieved without relying on $\left(\frac{p}{m_q}\right)^2$ corrections which in the EEM would probably allow one to get a similar result. Indeed, the orthogonality of wave functions, which explains the low transition rates given in table 3, does not apply anymore when the operator nature of these corrections is accounted for.

The overall results for the three potentials do not differ very much. Added to the $NN\pi$ form factor prediction and keeping in mind that other corrections, as the ones coming from the Δ -width in the final states, could be evaluated, the small remaining discrepancies with experimental data might then have to do with a fine tuning improvement of the quark potential on the base of increasing the quark model radii.

5 Summary

A refinement of a non-relativistic quark model that by means of the incorporation of a three quark potential is able to reproduce the nucleon and delta low energy spectra has been carried out avoiding some conceptual difficulties associated to the very singular form of the three-body force and to the values of the potential parameters in the original version. The predictions for static properties point out the need of incorporating $(qqq q\bar{q})$ components into the wave function. An effective manner to do this when studying strong decay processes is through the transition operator defining the calculation scheme either via a modification of the coupling constant as in a elementary emission model (EEM) or additionally via the explicit implementation of $q\bar{q}$ pair creation as in the quark pair creation models (QPCM).

We do find some sensitivity to the way the π -decay process occurs at the microscopic level. So the 3P_0 QPCM largely overestimates majority of the decay rates. Discrepancies were found to have an origin in relativistic effects. Starting from this observation, the QPCM was modified by incorporating those corrections which stem from general principles, making it closer to the EEM. The quality of the results we thus obtain seems to support our prescription. Despite large differences in the short distance description of baryons used in our calculations, we did not find any reason to discriminate them by looking at the π decay properties once the experimental kinematics is considered. Introducing a three body force in the description of baryons makes the agreement with experiment slightly better in some cases, slightly worse in others. Probably, the observable we examined is not appropriate to extract any correlation between the predictions for the spectrum and the decay widths. Anyhow as a general conclusion it can be established that a unified description of the spectrum and the strong baryonic decays in a 'non-relativistic' scheme seems plausible.

This work has been partially supported by CICYT under grant AEN93-0234 and by DGICYT under grant PB91-0119-C02-01. F.C. acknowledges the Ministerio de Educación y Ciencia for a FPI fellowship. B. D. has been partially supported by Conselleria d'Educació y Ciència of the Generalitat Valenciana.

Appendix A

All we can know about the baryonic structure is contained in the intrinsic wave function $\Psi(\vec{\xi}_1, \vec{\xi}_2)$ depending on the six independent coordinates $\vec{\xi}_1, \vec{\xi}_2$. Alternatively one can define hyperspherical coordinates in the dimension 6-hyperspace as an hyperradius ξ defined through

$$\xi^2 = \vec{\xi}_1^2 + \vec{\xi}_2^2 \quad (\text{A.1})$$

an a set Ω of 5 angles: $\hat{\xi}_1$ (the spherical angles of $\vec{\xi}_1$), $\hat{\xi}_2$ (the spherical angles of $\vec{\xi}_2$), and ϕ given by

$$\begin{aligned} \xi_1 &= \xi \sin \phi \\ \xi_2 &= \xi \cos \phi \end{aligned} \quad (\text{A.2})$$

such that $d\vec{\xi}_1 d\vec{\xi}_2 = d\xi \xi^5 d\Omega = d\xi \xi^5 d\phi \sin^2 \phi \cos^2 \phi d\hat{\xi}_1 d\hat{\xi}_2$

In terms of Ω one can construct a complete set of basis functions on the hypersphere unity. There are the hyperspherical harmonics (HH) $Y_{[K]}(\Omega)$, characterized by 5 quantum numbers denoted by $[K] \equiv [K, l_1, m_1, l_2, m_2]$ [9].

Then the spatial part of the intrinsic wave function can be expanded as:

$$\Psi(\vec{\xi}_1, \vec{\xi}_2) \equiv \Psi(\xi, \Omega) = \sum_{[K]} \Psi_{[K]}(\xi) Y_{[K]}(\Omega) \quad (\text{A.3})$$

satisfying the Schrödinger equation:

$$(H_{\text{int}} - E)\Psi(\xi, \Omega) = 0 \quad (\text{A.4})$$

where H_{int} stands for the sum of the internal kinetic and the potential energy.

Explicitly by defining reduced radial wave functions as

$$\psi_{[K_i]}(\xi) = \xi^{5/2} \Psi_{[K_i]}(\xi) \quad (\text{A.5})$$

and defining the wave function vector

$$\psi = \begin{pmatrix} \psi_{[K_1]} \\ \vdots \\ \psi_{[K_n]} \end{pmatrix} \quad (\text{A.6})$$

one has the set of coupled Schrödinger equations:

$$\left\{ \frac{1}{2m} \left(\frac{\partial^2}{\partial \xi^2} - \frac{\nu_K}{\xi^2} \right) - V + E \right\} \psi(\xi) = 0 \quad (\text{A.7})$$

where V is the matrix of the potential

$$V_{ij} = \langle Y_{[K_i]}(\Omega) | V(\xi, \Omega) | Y_{[K_j]}(\Omega) \rangle \quad (\text{A.8})$$

and ν_K is the diagonal matrix

$$(\nu_K)_{ij} = \left[(K_i + 2)^2 - \frac{1}{2} \right] \delta_{ij} \quad (\text{A.9})$$

The set of eqs. (A.7) can be solved numerically by Numerov integration, turning out to be convenient the introduction of the dimensionless variable:

$$x = \frac{\sqrt{2}m\xi}{\hbar c} \quad (\text{A.10})$$

in terms of which we can finally write

$$\left\{ -\frac{d^2}{dx^2} - \frac{\nu_K}{x^2} + \frac{V(x)}{m} - \frac{E}{m} \right\} \chi(x) = 0 \quad (\text{A.11})$$

Let us note that under a variation of the quark mass $m \rightarrow m'$ ($x \rightarrow x' = \frac{m'}{m}x$) (A.11) transforms into:

$$\left\{ -\frac{d^2}{dx'^2} - \frac{\nu_K}{x'^2} + \frac{\bar{V}(x')}{m'} - \frac{E'}{m'} \right\} \tilde{\chi}(x') = 0 \quad (\text{A.12})$$

where

$$\bar{V}(x') \equiv \frac{m}{m'}V(x) \quad (\text{A.13})$$

$$E' \equiv \frac{m}{m'}E \quad (\text{A.14})$$

$$\tilde{\chi}(x') \equiv \chi(x) \quad (\text{A.15})$$

So, by redefining the parameters of the potential to satisfy (A.13) we can obtain an energy spectrum rescaled by a factor $\frac{m}{m'}$ without any change in the wave functions.

For physical purposes it is more convenient to use linear combinations of HH with total orbital angular momentum L and definite symmetry, $Y_{[K,\text{symmetry}]}^{(L,M)}(\Omega)$ in terms of which the total intrinsic wave function reads:

$$\begin{aligned} [\Psi_B(\vec{\xi}_1, \vec{\xi}_2)\Phi_B(S, M_S; I, M_I)]_{JJ_z} &= \sum_i \Psi_{B_i}(\xi) \left[\sum_{[\text{symmetry}]} (L_i S_i J | M_i M_{S_i} J_z) \cdot \right. \\ &\quad \left. Y_{[K_i,\text{symmetry}]}^{(L_i, M_i)} \Phi_{[\text{symmetry}]}(S_i, M_{S_i}; I_i, M_{I_i}) \right] \quad (\text{A.16}) \end{aligned}$$

having to be totally symmetric as required by the symmetrization postulate.

References

- [1] J.J.J. Kokkedee, The Quark Model (Benjamin, 1969).
F.E. Close, An Introduction to Quarks and Partons, (Academic Press, 1979).
- [2] A. De Rújula H. Georgi and S.L. Glashow, Phys. Rev. D12 (1975) 147.
- [3] N. Isgur and G. Karl, Phys. Rev. D18 (1978) 4187; D19 (1979) 2653; D20 (1979) 1191.

- [4] B. Silvestre–Brac and C. Gignoux, *Phys. Rev.* D32 (1985) 743.
R.K. Bhaduri, L.E. Cohler and Y. Nogami, *Nuovo Cimento* A65 (1981) 376.
- [5] B. Desplanques, C. Gignoux, B. Silvestre–Brac, P. González, J. Navarro and S. Noguera, *Z. Phys.* A343 (1992) 331.
- [6] R.K. Bhaduri, L.E. Cohler and Y. Nogami, *Phys. Rev. Lett.* 21 (1980) 1369.
- [7] Particle Data Group, *Phys. Rev.* D50 (1994) 1173.
- [8] F. Fernández, A. Valcárce, U. Straub and A. Faessler, *J. Phys.* G19 (1993) 2013.
- [9] J.L. Ballot and M. Fabre de la Ripelle, *Ann. Phys.* 127 (1980) 62.
- [10] V. Vento, *Phys. Lett.* 121B (1983) 370.
S.A. Chin and G.A. Miller, *Phys. Lett.* 121B (1983) 232.
- [11] D. Faiman and A.W. Hendry, *Phys. Rev.* 180 (1969) 1572.
- [12] A. Le Yaouanc, L. Oliver, O. Pène and J.-C. Raynal, *Hadron Transitions in the Quark Model* (Gordon and Breach Science Publishers, 1988).
- [13] A. Mitra and M. Ross, *Phys. Rev.* 158 (1967) 1630.
- [14] R. Koniuk and N. Isgur, *Phys. Rev.* D21 (1980) 1868.
S. Capstick and W. Roberts, *Phys. Rev.* D47 (1993) 1994.
- [15] E. Oset, H. Toki and W. Weise, *Phys. Rep.* C83 (1983) 281.
- [16] A. Le Yaouanc, L. Oliver, O. Pène and J.-C. Raynal, *Phys. Rev.* D8 (1973) 2223; D11 (1975) 1272.
- [17] R.K. Bhaduri, *Models of the Nucleon, Lecture Notes and Supplements in Physics* (Addison–Wesley Publishing Company, 1988).

Table captions

Table 1. Fitted values of the parameters of the two-body and three-body potentials.

Table 2. Magnetic moments (in nuclear magnetons) and radii (if fm²) of the nucleon.

Table 3. Decay widths (in MeV) with an EEM model. Experimental data from [7].

Table 4. Values of γ obtained from the $NN\pi$ vertex.

Table 5. Decay widths (in MeV) with a 3P_0 model. Pion wave function as given by eq. (31) and γ taken from table 4.

Table 6. Decay widths (in MeV) with a modified 3P_0 QPCM. Pion wave function given by eq. (31).

Figure captions

Figure 1. Relative energy spectrum for positive parity nucleon and delta and negative parity nucleon states. Solid lines correspond to the predictions of V_I and the shaded region whose size represents the experimental width to the experimental data [7].

Figure 2. Idem fig. 1 with $V_I \rightarrow V_{II}$.

Figure 3. Idem fig. 1 with $V_I \rightarrow V_{III}$.

Figure 4. Spatial symmetric component of the nucleon reduced wave function $\psi_1(\xi)$. The solid line corresponds to V_I , the dashed-dot line to V_{II} and the dashed line to V_{III} .

Figure 5. A baryon B decays through pion emission by one of its quarks.

Figure 6. Normalized $NN\pi$ form factor. The dot line corresponds to the phenomenological parameterization of ref. [15]. The solid line, dashed-dot and dashed line correspond to the predictions of V_I , V_{II} and V_{III} respectively.

Figure 7. A quark and antiquark from the vacuum recombine with the quarks of the initial baryon to give rise to the final baryon and pion.

Figure 8. Normalized pion wave function. The solid line is obtained from the Fourier transform of the pion form factor (32) The dashed line corresponds to the gaussian form eq. (31).

Figure 9. Normalized $NN\pi$ form factor in the 3P_0 model. The line corresponds to the phenomenological parameterization of ref. [15]. For the pion wave function, eq. (31) with $R_A^2 = 8 \text{ GeV}^{-2}$.

		V_I	V_{II}	V_{III}
$m_u = m_d$ (GeV)		0.337	0.355	0.320
$V^{(\text{COUL})}$	κ (GeV fm)	0.1027	0.289	0.321
$V^{(\vec{\sigma}\vec{\sigma})}$	κ_σ (GeV fm)	0.1027	0.049	0.044
	r_0 (fm)	0.4545	0.40	0.49
$V^{(\text{CONF})}$	a^2 (GeV ⁻¹ fm)	1.063	4.570	4.124
$V_I^{(3)}$	V_0 (GeV ⁻² fm ⁻⁶)	–	-61.63	–
	m_0 (GeV)	–	0.25	–
$V_{II}^{(3)}$	V_0 (GeV)	–	–	-35.5
	λ (fm)	–	–	0.25

Table 1

	V_I	V_{II}	V_{III}	Exp.
μ_p	2.76	2.64	2.93	2.79
μ_n	-1.83	-1.76	-1.95	-1.91
$\langle r_N^2 \rangle_m$	0.218	0.128	0.115	
$\langle r_p^2 \rangle_{Ch}$	0.238	0.133	0.112	0.74 ± 0.02
$\langle r_n^2 \rangle_{Ch}$	-0.02	-0.005	-0.004	-0.119 ± 0.004

Table 2

	V_I	V_{II}	V_{III}	Exp.
$\Delta(1232) \rightarrow N\pi$	79.6	72.1	67.7	115–125
$N(1440) \rightarrow N\pi$	3.4	0.17	0.01	210–245
$N(1440) \rightarrow \Delta\pi$	7.1	17.6	24.1	70–105
$\Delta(1600) \rightarrow N\pi$	20.1	94.1	148.6	35–88
$\Delta(1600) \rightarrow \Delta\pi$	2.85	0.10	0.08	140–245
$N(1520) \rightarrow N\pi$	61.8	22.3	17.8	60–72
$N(1520) \rightarrow \Delta\pi$	78.0	56.1	55.3	18–30
$N(1535) \rightarrow N\pi$	240	149	117	53–83
$N(1535) \rightarrow \Delta\pi$	9.7	8.3	9.1	<1.5

Table 3

	V_I	V_{II}	V_{III}
γ	7.02	9.78	11.04

Table 4

	V_I	V_{II}	V_{III}	Exp.
$\Delta(1232) \rightarrow N\pi$	167	210	241	115–125
$N(1440) \rightarrow N\pi$	452	1076	1509	210–245
$N(1440) \rightarrow \Delta\pi$	66.5	228	337	70–105
$\Delta(1600) \rightarrow N\pi$	19.8	0.53	7.0	35–88
$\Delta(1600) \rightarrow \Delta\pi$	255	498	656	140–245
$N(1520) \rightarrow N\pi$	268	319	353	60–72
$N(1520) \rightarrow \Delta\pi$	532	999	1203	18–30
$N(1535) \rightarrow N\pi$	429	464	410	53–83
$N(1535) \rightarrow \Delta\pi$	28.1	74.0	107	<1.5

Table 5

	V_I	V_{II}	V_{III}	Exp.
$\Delta(1232) \rightarrow N\pi$	88.6	112	123	115–125
$N(1440) \rightarrow N\pi$	114	307	469	210–245
$N(1440) \rightarrow \Delta\pi$	27.6	116	183	70–105
$\Delta(1600) \rightarrow N\pi$	2.1	2.5	5.6	35–88
$\Delta(1600) \rightarrow \Delta\pi$	62.0	121	177	140–245
$N(1520) \rightarrow N\pi$	95.1	105	118	60–72
$N(1520) \rightarrow \Delta\pi$	45.9	75.2	111	18–30
$N(1535) \rightarrow N\pi$	49.2	44.1	55.8	53–83
$N(1535) \rightarrow \Delta\pi$	15.3	36.3	52.1	<1.5

Table 6

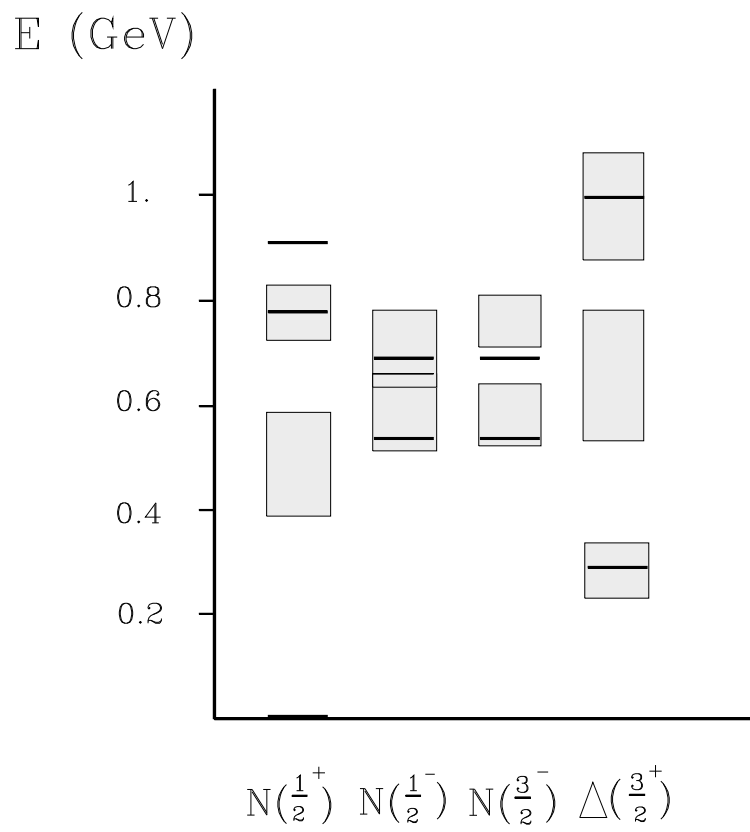


Fig. 1

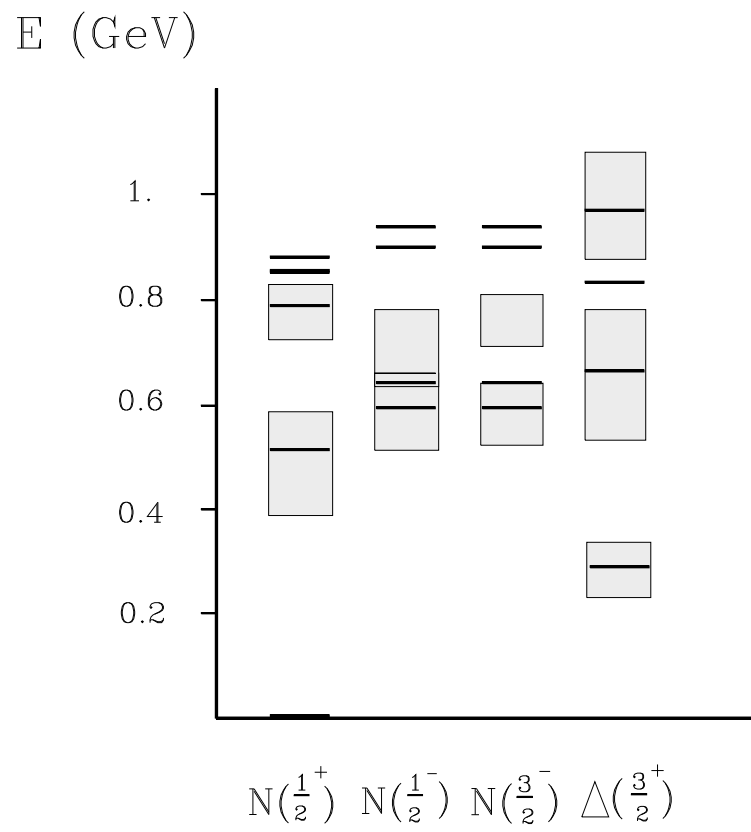


Fig. 2

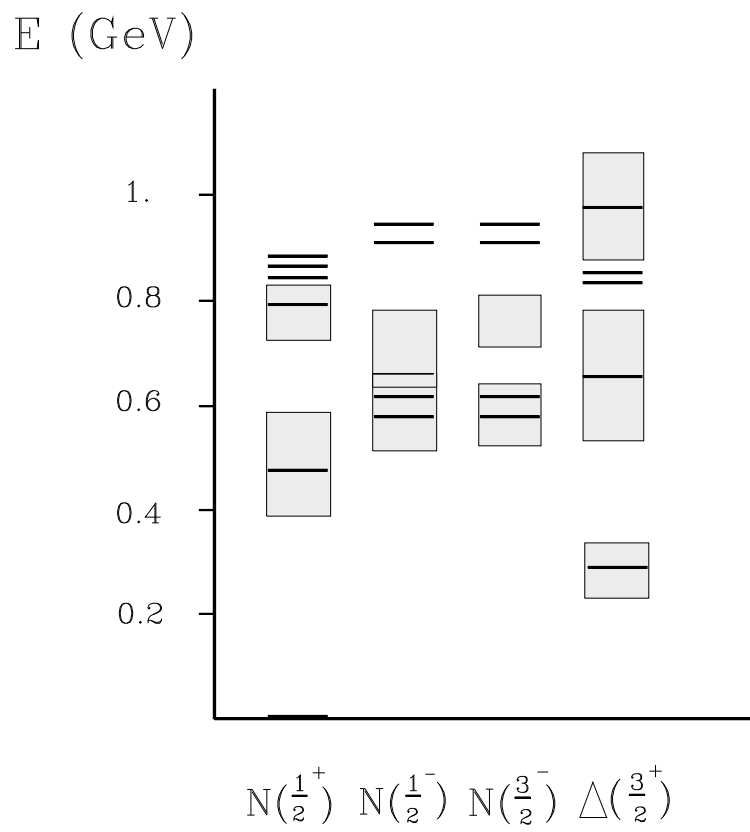


Fig. 3

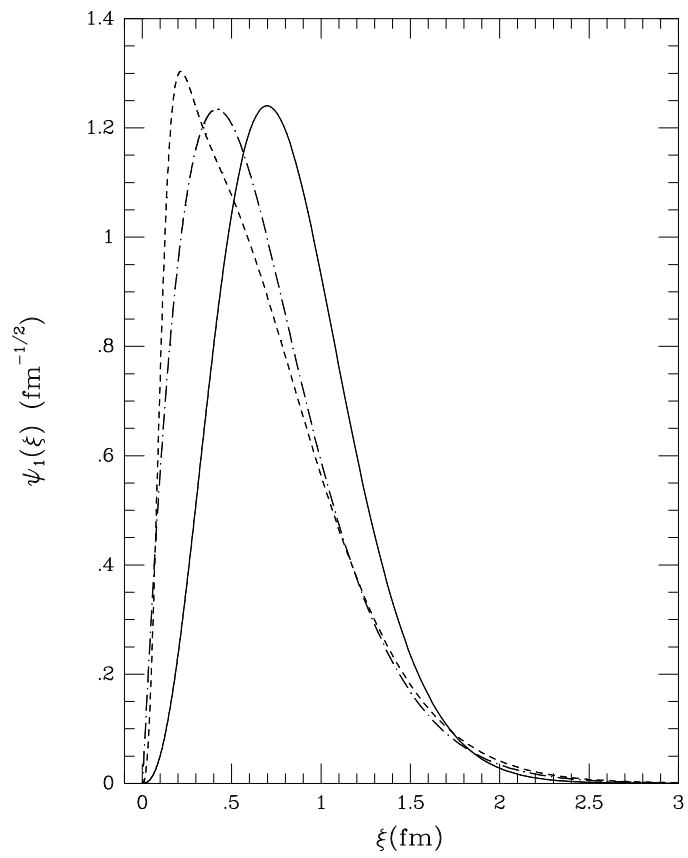


Fig. 4

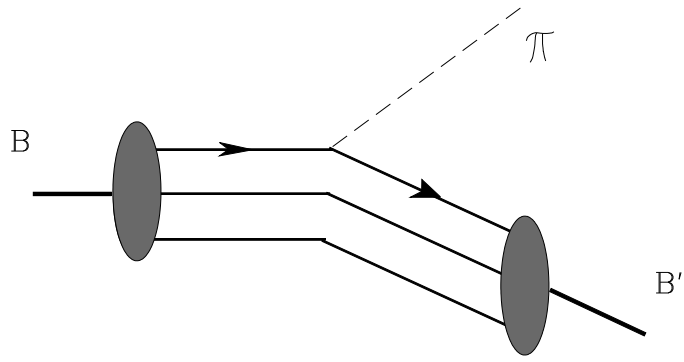


Fig. 5

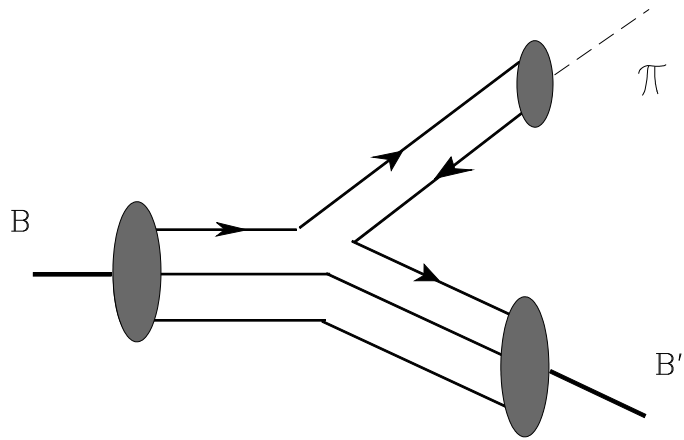


Fig. 7

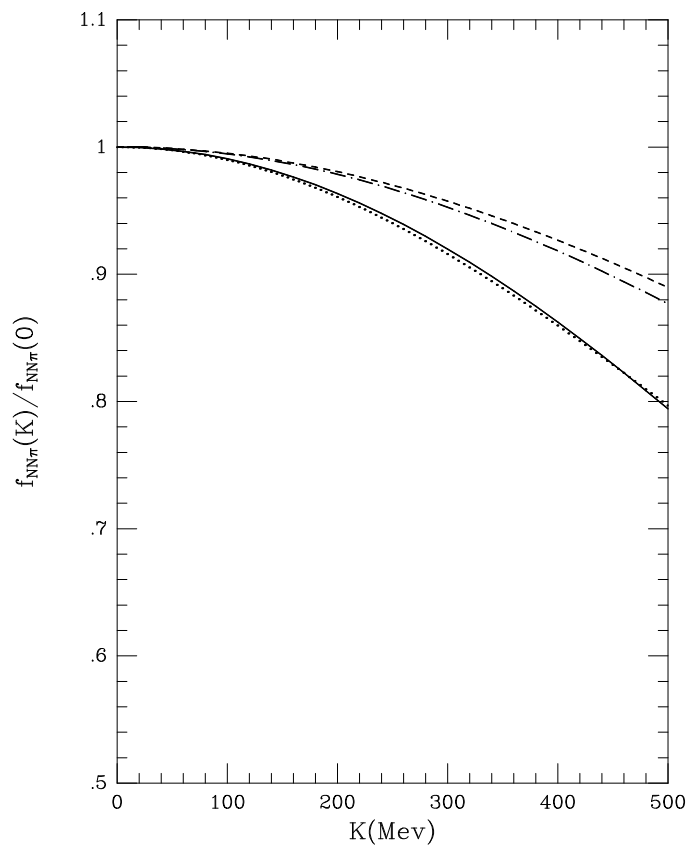


Fig. 6

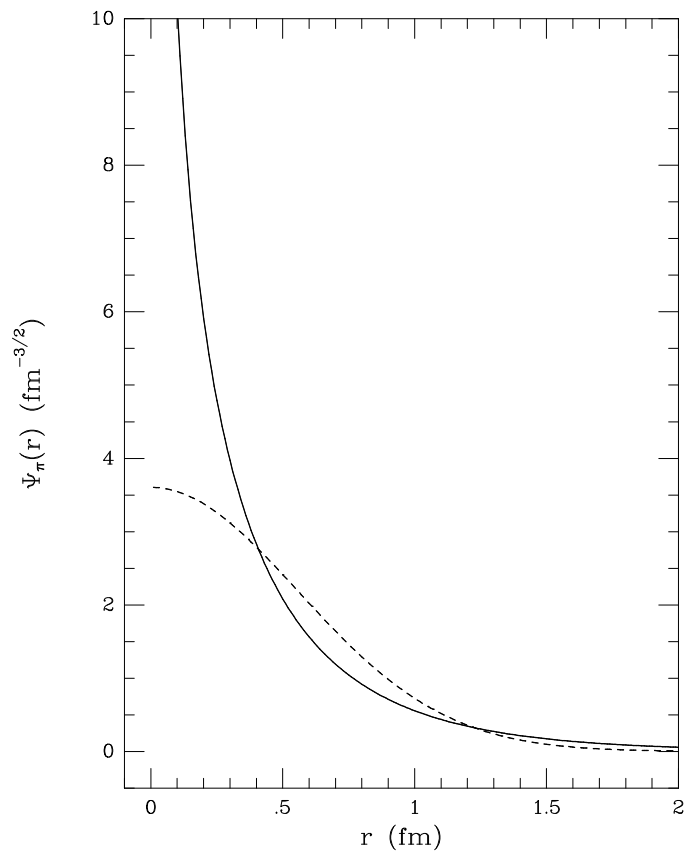


Fig. 8

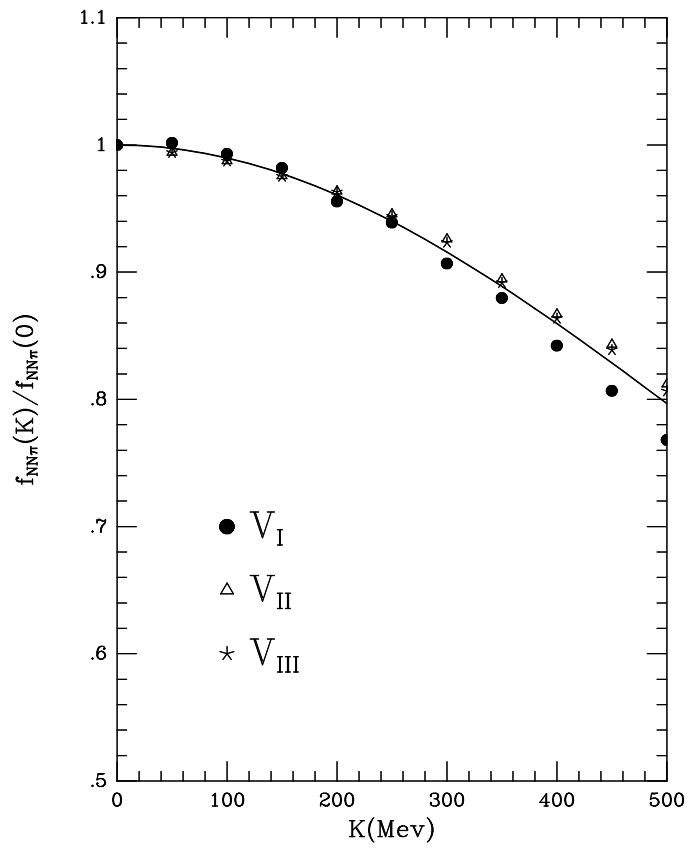


Fig. 9